Available online at www.sciencedirect.com
SCIENCE DIRECT®

International Journal of Heat and Fluid Flow 24 (2003) 421–430

International Journal of HEAT AND FLUID FLOW

www.elsevier.com/locate/ijhff

The effect of negative shear on the transitional separated flow around a semi-circular leading edge

A. Palikaras, K. Yakinthos, A. Goulas *

Department of Mechanical Engineering, Laboratory of Fluid Mechanics and Turbomachinery, Aristotle University of Thessaloniki, 54 124, Thessaloniki, Greece

Received 10 August 2002; accepted 3 December 2002

Abstract

The effect of a negative free-stream mean-shear velocity distribution on the boundary layer development on a flat plate with a semi-circular leading edge is studied experimentally and computationally. The geometry is the same as in the T3L test case of the ERCOFTAC Special Interest Group on Transition. The existence of a negative shear is related to the transition of the boundary layer from laminar to turbulent through separation. The flow investigated here has the same general characteristics as the one presented in a recent work by the authors, Palikaras et al. [Int. J. Heat Fluid Flow 23 (2002) 455–470], where the boundary layer development has been studied under free-stream conditions of uniform and positive mean-shear velocity distributions. The negative shear flow in the core region of the wind tunnel has a value $\partial\overline{U}/\partial y = -27.7\ \mathrm{s}^{-1}$, which is the opposite to the case examined by Palikaras et al. [Int. J. Heat Fluid Flow 23 (2002) 455–470]. In the first part of the paper, a detailed description of the flow is given. The measured quantities are presented, discussed and compared with the computational analysis in order to obtain a complete picture of the investigated flow. For the computations, the non-linear k–ε model of Craft et al. [Int. J. Heat Fluid Flow 17 (1996) 108–115] is used, and satisfactory predictions are reported. In the second part, a detailed comparison of the results with the cases of uniform and positive mean-shear velocity inlet distribution is carried out. In the case of negative mean velocity the separated boundary layer leads to a larger reverse flow region than the two other cases. A relation is observed between the location of the stagnation point at the leading edge and the presence or absence of shear. When mean shear is present, depending on the sign, there is a movement of the stagnation point away from the symmetry line of the flat plate and it is believed that this is the driving mechanism that affects the boundary layer development and the longitudinal size of the reverse flow region. This remark is supported by the observation that for all the three cases studied, the longitudinal RMS distribution above the reverse flow region and in the free-stream region has the same values.

Keywords: Transition; Separation; Positive/negative mean shear; Turbulence modeling; Non-linear eddy viscosity model

1. Introduction

Among the various phenomena appearing in a fluid flow, boundary layer transition from a laminar to a turbulent state is the most difficult one to describe, control and predict. According to Mayle (1991), transition occurs through three basic modes reported as: natural, by-pass and through boundary layer separation. All of them are affected primarily by the free-stream turbulence (FST) and pressure gradient. In the research community, the work that has been carried out until now has been primary focused on the effect of FST, free-stream velocity and pressure gradient for the natural and by-pass transition on thin flat plates where the boundary layer development was examined experimentally and computationally (ERCOFTAC SIG on transition). Besides a Reynolds number dependency it has been shown that higher FST values accelerate transition (when boundary layer separation is not present). Strong adverse pressure gradients also accelerate transition. For transition through boundary layer separation, experimental investigations on flat plates having various leading edge shapes have also been carried out. It was clearly shown that the separation of the boundary layer and the size of the reverse flow region was related to the

* Corresponding author. Tel.: +30-0310-99-6001; fax: +30-0310-99-6002.

E-mail addresses: achille@eng.auth.gr (A. Palikaras), kyros@eng.auth.gr (K. Yakinthos), goulas@eng.auth.gr (A. Goulas).

0142-727X/03/$ - see front matter © 2003 Elsevier Science Inc. All rights reserved.
doi:10.1016/S0142-727X(02)00240-0

Nomenclature

H	shape factor
k	turbulence kinetic energy
k_0	turbulence kinetic energy at the inlet
l	dissipation rate length scale in the free-stream or at the inlet region
L	length of the reverse flow region
R	leading edge radius ($R = 5$ mm)
Re_θ	Reynolds number based on boundary layer momentum thickness
$\overline{U}$	mean velocity
U_c	inlet velocity at the center line of the wind tunnel (symmetry line), equals to 5 m/s for the three examined cases
U_{max}	maximum velocity in a boundary layer velocity distribution (located at the edge of the boundary layer)
u	local velocity (measured or computed) in every station
$\overline{u'u'}$, $\overline{v'v'}$	Reynolds stresses (x and y-component resp.)
u'	root mean square (RMS) value of the fluctuating longitudinal (x-component) velocity component

Greeks

δ^*	boundary layer displacement thickness
ε	dissipation rate of k
ε_0	dissipation rate of k at the inlet
θ	boundary layer momentum thickness
μ	dynamic viscosity

leading edge geometry and affected the transition mechanism (Savill, 1995). Transition through separation takes place in the free shear layer, and this can either be natural or by-pass transition. Generally, the flow in a separated boundary layer is more susceptible to disturbances. The turbulent spot production rate is much stronger near the separation point than that in the attached boundary layers which leads to shorter transition lengths.

Palikaras et al. (2002) proceeded to further investigation of transition on a flat plate with a semi-circular leading edge under two different free-stream velocity distributions. The first one had a uniform inlet velocity, while the second had an inlet velocity distribution with positive shear. The value of the positive shear was $\partial\overline{U}/\partial y = 27.7\ \mathrm{s}^{-1}$ while the upstream velocity at the axis of symmetry of the plate was in both cases equal to 5 m/s. The corresponding Reynolds number based on the leading edge diameter had the value of 3304. The average FST level (at a non-dimensional distance $x/R_{\text{leading edge}}$ equal to 15 upstream and on the symmetry line of the flat plate) was the same for both cases, 7%. It was shown that transition was developing through boundary layer separation that occurred on the flat section of the plate surface just beyond the leading edge. The size of the reverse flow region and thus, the transitional area, was affected by the free-stream conditions. The existence of positive shear led to a smaller reverse flow region compared to the uniform one both in thickness and length. These conclusions could not be shown very clearly experimentally since the measurement technique (hot-wire anemometry) imposed some limitations concerning the nearest to the wall measurement point. On the other hand it was not possible to measure the negative values of velocity inside the region of the separated boundary layer. It is well known that the classic hot-wire anemometry technique in general does not indicate the sign of velocity. Concerning the measurements with the hot-wire anemometry of the longitudinal Reynolds stresses $\overline{u'u'}$, the values are correct, within the error band indicated, when the instantaneous velocity has the same sign. In a region close to stagnation point where the instantaneous velocity during a time record can have opposite signs, because of the rectification of the signal, the mean velocity is overestimated. The RMS thought (root mean square value which is used to calculate explicitly the Reynolds stress), being the square root of the square of differences, remains the same and therefore correct within the error band of the measurement. Thus, concerning the velocity field, there is a need to use a computational approach to clarify how the flow developed especially in the separation region where the velocity has a negative sign. Regarding the development of the flow in the free-stream region, although a monotonic growth of the Reynolds stresses (for the cases where shear was present) was observed, a detailed analysis of the stresses above the boundary layer and in the neighborhood of the reverse flow region has shown that the longitudinal Reynolds stresses have almost the same values and within the same error band for both the uniform and positive shear free-stream velocity distribution.

In this work, the effect on the flow development, when a negative mean shear free-stream velocity distribution is imposed, is presented. The experimental data are also compared with those obtained for uniform and positive shear free-stream velocity distributions.

2. Experimental apparatus

The experimental apparatus is exactly the same as the one described by Palikaras et al. (2002). A flat plate having a thickness of 10 mm and a shaped semi-circular leading edge is placed in a wind tunnel. The boundary layer development is studied on the horizontal (flat) section of the plate surface. Various inlet conditions for the FST, the velocity magnitude and velocity distribution can be obtained using turbulence grid generators, appropriate blower speed and shaped shear generators. Extra care was taken to have the same wind tunnel conditions, i.e., location of the measurement stations, average FST level values (equal to 7%), center-line velocity value (equal to 5 m/s) and flat plate positioning inside the wind-tunnel, in order to be able to make a full comparison with the other two already studied cases. The value of the mean shear applied was $\partial \overline{U}/\partial y = -27.7\ \mathrm{s}^{-1}$. The measurements have been carried out using the hot-wire anemometry technique. Details on the measurement procedure, measurement stations and measurement error analysis can be found in Palikaras et al. (2002).

3. Computational approach

Computations corresponding to the experiments were carried out by means of CFD using an in-house elliptic Navier–Stokes solver. The purpose of the computations was not to test some of the existing turbulence models, but rather to obtain supporting information about the flow development. The non-linear k–ε model of Craft et al. (1996) was adopted for the turbulence modeling. To avoid an unstable convergence behavior, the solver started the iterative procedure with a linear eddy viscosity k–ε low Reynolds number turbulence model (the classical Launder–Sharma) and after some preliminary iterations it switched to the non-linear eddy-viscosity model. Details on the computational procedure can also be found in Palikaras et al. (2002).

4. Experimental and computational results

First, measurements in the free-stream region to check the velocity distribution downstream of the leading edge of the plate were carried out. Fig. 1 shows the velocity profiles where it can be seen that the velocity gradient (shear) remains nearly constant along the plate. The non-dimensional distance x/R refers to the downstream location beyond the leading edge of the flat plate and R is the radius of the leading edge, equal to 5 mm. The inlet station is located at $x/R = -30$ while $x/R = 0$ corresponds to the first point on the leading edge of the flat plate.

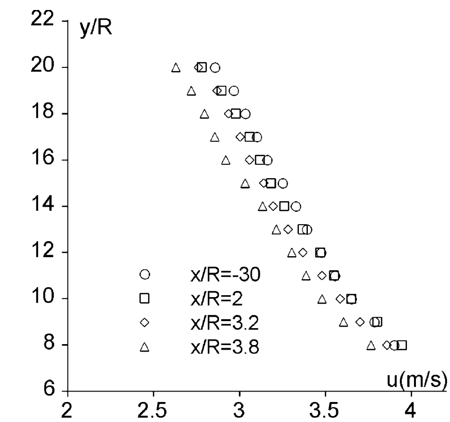

Fig. 1. The velocity gradient away from the plate surface for various stations downstream the flow.

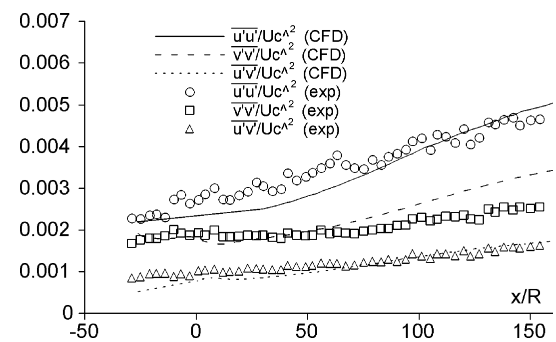

Fig. 2. Downstream evolution of $\overline{u'u'}$, $\overline{v'v'}$ and $\overline{u'v'}$ for negative shear velocity distribution. Experimental data and computational results.

Fig. 2 shows the distribution of the Reynolds stresses in the streamwise direction within the free-stream. A monotonic growth due to the presence of the negative shear is indicated. In the same figure, the computational results obtained by adopting an appropriate turbulence dissipation rate, are also given. The stresses are non-dimensionalized using the velocity at the center line at the inlet of the wind tunnel, U_c, which is equal to 5 m/s. These measurements are located at a normal distance $y/R = 15$ from the surface of flat plate in the downstream direction. They have been carried out in order to obtain information on the development of the Reynolds stresses and use it for comparison of the FST between experiment and computations. This specific distance is located in a region where the velocity gradient remains constant and equal to the value at the inlet, which as shown in Fig. 1, extends to y/R between 7 and 20.

The velocity distributions at various stations downstream of the leading edge and its comparison with the computational ones is presented in Fig. 3. The values of the velocity are non-dimensionalized by the maximum velocity appearing for *each measurement station* at the edge of the boundary layer. For the cases where mean shear is present, the edge of the boundary layer was

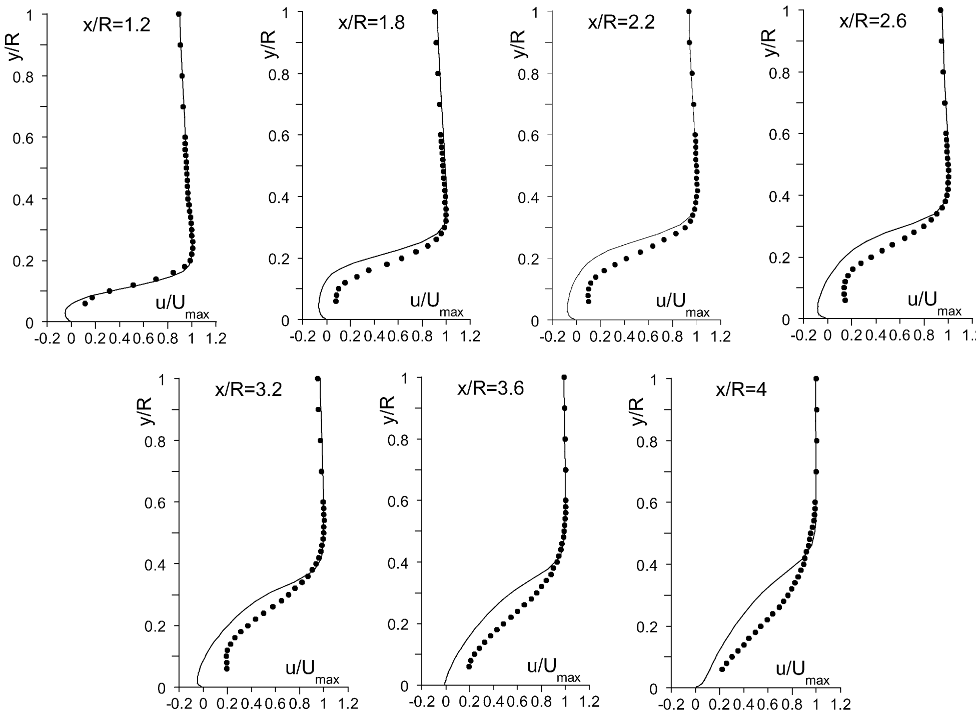

Fig. 3. Velocity profiles at seven stations. Experimental data: dots, computational results: plain line.

considered to be the point where the velocity gradient within the boundary layer obtains the same value with the free-stream at the same x station. Because of the limitations of the hot-wire anemometry technique discussed in the introduction, the sign of reverse flow cannot be indicated. One though can identify the region of reverse flow as the area towards the wall below the inflection point of the measured velocity profile. In the region where the flow is attached, $x/R = 3.6$, the experimental data tend smoothly to the wall. It must be pointed here that the measured here velocity distribution *inside the boundary layer and especially in the region where the flow is separated*, has similar behavior, concerning the "false" values (measured by the hot-wire technique as positive although they have negative values) and the sudden change of gradient, to those measured and reported by Lou and Hourmouziadis (2000) for a separated boundary layer under the influence of a positive pressure gradient.

For the computations, a characteristic length scale l is required in order to calculate the inlet value of ε_0 by using the following formula:

$$\varepsilon_0 = k_0^{3/2}/l \quad (1)$$

The values of the inlet turbulence kinetic energy, k_0, were obtained from the experimental data. For the present results l was set to an average value equal to 30 mm. Numerical experiments showed that this value gave in general the best agreement between computed and experimental Reynolds stresses in the free-stream region. At this point it is worth to note that the choice of ε_0 has been found by many researchers to be very crucial. Chen et al. (1998) reported that the specification of the characteristic length scale (and thus of the turbulence dissipation rate) is most of the times unknown and requires careful consideration. They suggested that for a standard wind tunnel flow the value of l can be determined by computational experiments in order to match the computational free-stream decay with the experimental one, see also Palikaras et al. (2002). In other cases, such as the external flow over an airfoil, see Apsley and Leschziner (1998), l was determined in relation to the chord length (a priori chosen to a specific value). Thus, it is true that the determination involves some empiricism when detailed experimental data cannot be provided. In this work, when shear is present, a more detailed analysis must be performed since one expects that the length scale should be variable. Based on these remarks and since the scope of the computational part of this work is concentrated to the support of the experiments, it was considered appropriate to carry out computational experiments to find an average value of length scale in order to match as close as possible the values of the computed Reynolds stresses to the experimental ones in the free-stream region. Due to the non-uniform distribution of the experimental values of k at the inlet, the use of Eq. (1) leads implicitly to a variable turbulence dissipation rate at the inlet across the flow field.

The first observation coming out of the computations is that separation starts earlier than the first measurement station. There is a large reverse flow region that extends up to stations between $x/R = 3.2$ and 3.6 downstream of the stagnation point, something that is more clearly shown by reference to the computational results. The maximum height of the reverse flow region is about $y/R = 0.1$. The computations with the use of the non-linear k–ε model are in a satisfactory agreement with the experimental data, although a slightly longer, by about 0.5 mm (0.1 non-dimensionalized by R), reverse flow region is predicted.

The experimental data for the RMS (root mean square value of the longitudinal fluctuations) distributions and their comparison with the computational results are shown in Fig. 4. The maximum experimental RMS value is located at some distance from the plate's surface and this indicates the edge of the reverse flow region as a high shear flow. Away from the boundary the RMS drops asymptotically to the free-stream value which is about 0.1.

The maximum value of RMS for each station is located at a normal distance from the plate surface which is related to the position of maximum rate of production of turbulence. In the first three measurement stations, the region of maximum production of turbulence is confined into a small region. In the last two stations, where the flow has reattached, the region of high turbulence broadens to cover the full region of the boundary layer. At the stations located at $x/R = 1.2$, 2.2, 2.6 and 3.2 inside the boundary layer, a minimum value of RMS is observed which then increases again towards the wall. As it has already been mentioned, the non-dimensional height of the reverse flow region is approximately 0.1. This means that at least three measurement points are inside the reverse flow region. While the fluid is moving in the opposite to the mean flow direction a "second" boundary layer (its origin being the reattachment point) is developing close to the wall. For this reason the RMS, very close to the wall has a local maximum. As the flow in this region is in the opposite to the main flow direction the RMS starts with a high value close to the reattachment point related to the unsteadiness of the reattachment point, see Castro and Haque (1987), and its value is reduced in the direction of the flow. The computations give satisfactory results for the majority of the measurement stations but they are unable to resolve the local minimum in the RMS distribution close to the wall. The non-linear k–ε model behaves well although it has a tendency to slightly over predict the RMS values in the free shear layer. In Fig. 5 the boundary layer integral parameters are presented together with the computational results. Despite the limitations of the hot-wire technique based mainly in its inability to get accurate wall values, an attempt was made to investigate the development of these parameters. The values of the integral parameters close to the plate surface (where measurements could not be carried out) have been computed using a polynomial fitting. In

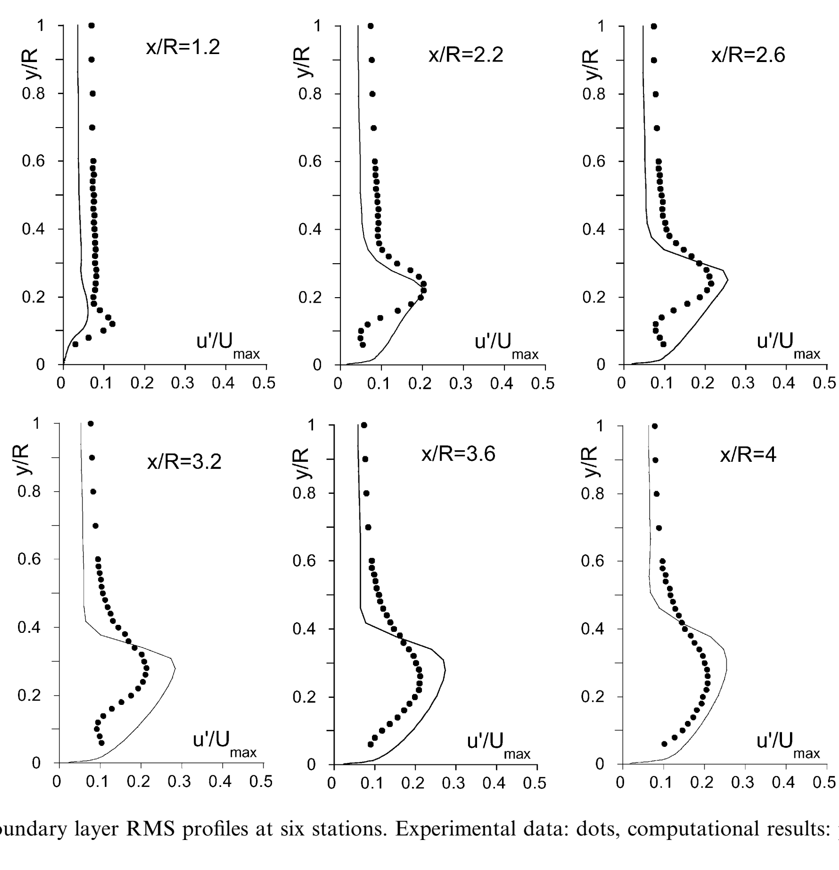

Fig. 4. Boundary layer RMS profiles at six stations. Experimental data: dots, computational results: plain line.

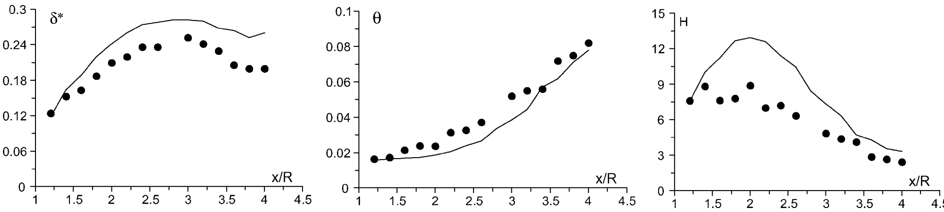

Fig. 5. Boundary layer integral parameters. Experimental data: dots, computational results: line.

this procedure the velocities in the region between $y/R = 0$ (flat plate surface) and y/R corresponding to the end of the reverse flow can be computed using a second order polynomial equation. The coefficients of this equation can be determined by setting the following conditions: $u_{y/R=0} = 0$ m/s, $u_{y/R=\text{end of reverse flow}}$ is equal to the measured velocity at the last point before the reverse flow region. The gradient $\mathrm{d}u/\mathrm{d}y$ needed for the polynomial fitting is computed taking into account the measured values of the velocity in the region between *y/R equals to the end of the reverse flow and the next measurement point.* So, *only for the polynomial fitting*, the first three or four measurements points from the wall (the number depends on the thickness of the reverse flow) corresponding to the reverse flow region are ignored. This procedure is applied for all the downstream measurement locations.

The shape factor H from downstream of $x/R = 2.4$ decreases and thus, the boundary layer tends to a fully turbulent flow regime. In the last measurement station, the value of the shape factor is about 2.3. In conventional fully turbulent zero-pressure-gradient boundary layers the characteristic value of the shape factor is approximately equal to 1.3. The computational results again, are generally in a satisfactory agreement with the experimental data.

5. The effect of mean shear

As already mentioned, the primary aim of this work was the study of the effect of negative shear on the boundary layer development and thus on transition through boundary layer separation. A comparison will be made with the cases of uniform free-stream and the positive shear free-stream inlet velocity distribution.

The development of the Reynolds stresses downstream at the same normal distance from the plate surface for the two cases of positive and negative shear is shown in Fig. 6. There is a monotonic increase of the $\overline{u'u'}$ and $\overline{v'v'}$ stresses, for both cases, the longitudinal gradient are nearly the same and the values are within the limits reported by Rohr et al. (1988) for a pure wind tunnel shear flow, although the values of the stresses for the negative shear are lower than the ones for the positive shear. Because both cases have the same mean

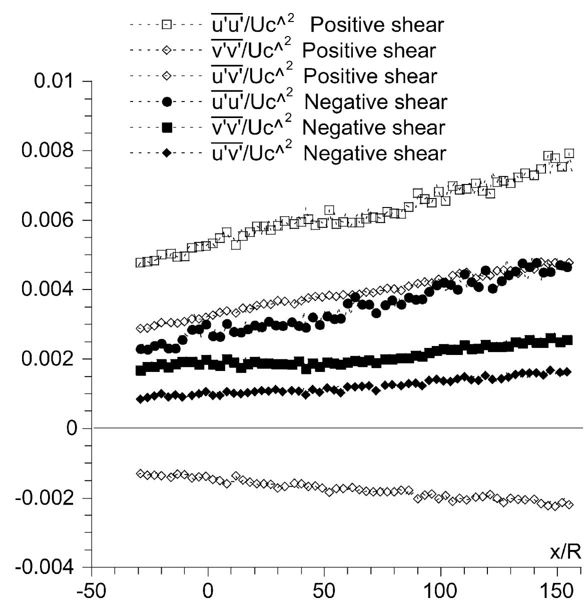

Fig. 6. Reynolds stresses downstream the fluid flow for positive and negative mean shear.

velocity gradient, the rate of production of turbulence is the same for both cases. The differences between the corresponding sets of curves are due to the different initial values of RMS which are affected by the gradient generation device, which has a variable solidity along the y direction. One should expect that these differences will affect the transitional boundary layer development through FST. It will be shown later that this is not the case, as the values in the region just above the reverse flow and the normal to the wall gradient of $\overline{u'u'}$ (which has a major role to the contribution to the FST) are nearly the same for all the three cases studied.

Fig. 7 shows the velocity distribution diagrams for a uniform inlet free-stream velocity, a positive mean shear free-stream velocity distribution as it was measured and reported by Palikaras et al. (2002) and the negative mean shear as is reported in the present work. For the three cases studied, the free-stream inlet velocity has a value equal to 5 m/s and a FST level equal to 7%, at the "center-line" which coincide with the symmetry line of the flat plate. The values of velocity are here again non-dimensionalized by the maximum velocity appearing for *each measurement station* at the edge of the boundary layer.

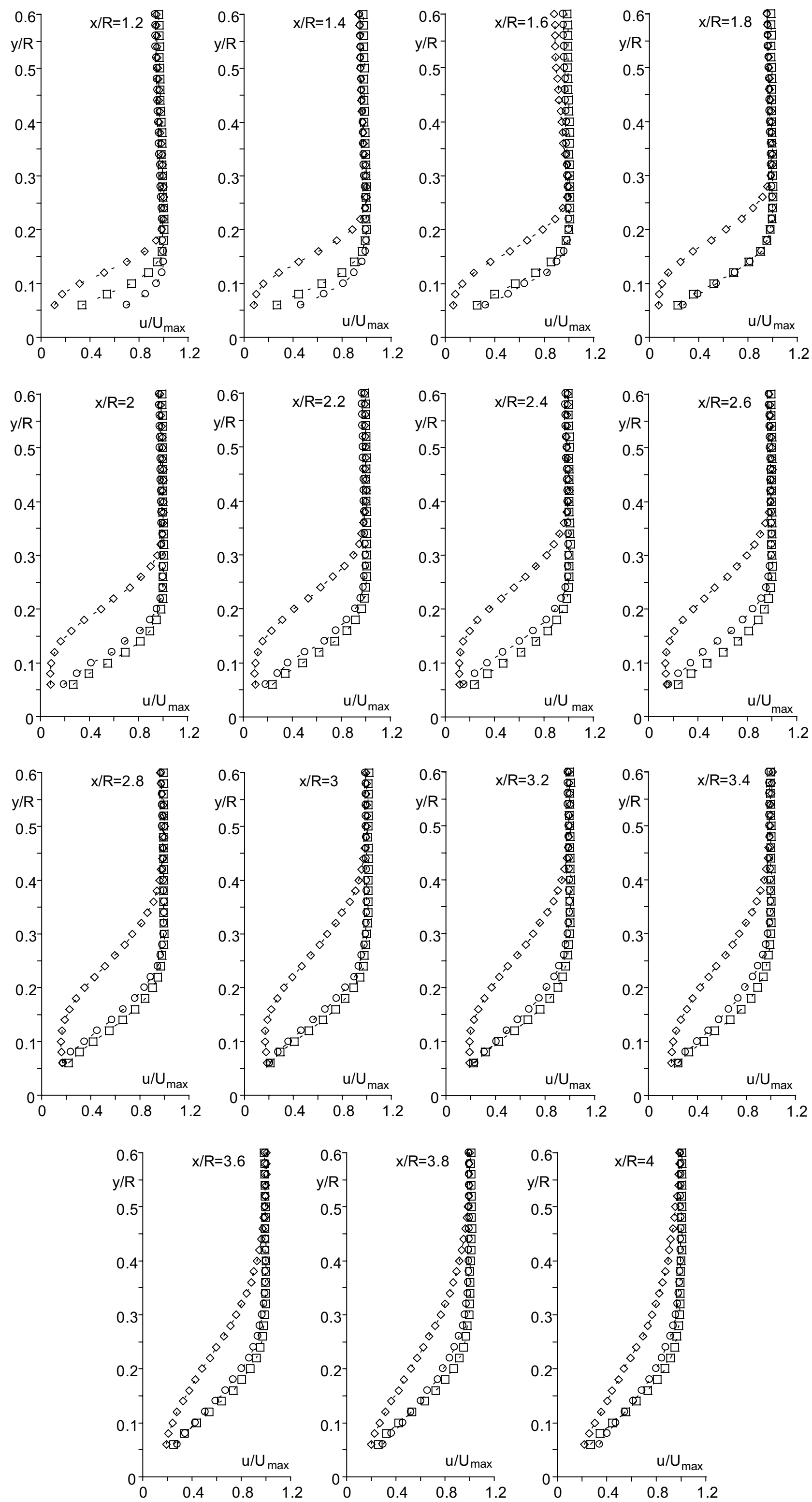

Fig. 7. Uniform free-stream inlet velocity distribution (circular symbols), negative mean shear (rhomboid symbols) and positive mean shear (rectangular symbols) free-stream inlet velocity distribution. Comparative boundary layer velocity profiles.

In the case of negative mean shear the presence of a large reverse flow region is clearly indicated. Comparing the three cases it can be concluded that the presence of a mean shear affects the boundary layer development and the size of the reverse flow region. The length of the reverse flow region (non-dimensionalized by the radius of the leading edge) as a function of the value of shear for the three cases is shown in Fig. 8. In the same figure, the computational results of the present work and those reported by Palikaras et al. (2002) are also shown. According to the experimental data, there is a linear relationship between the length of the reverse flow region and the mean-shear value. The negative shear leads to a larger reverse flow region.

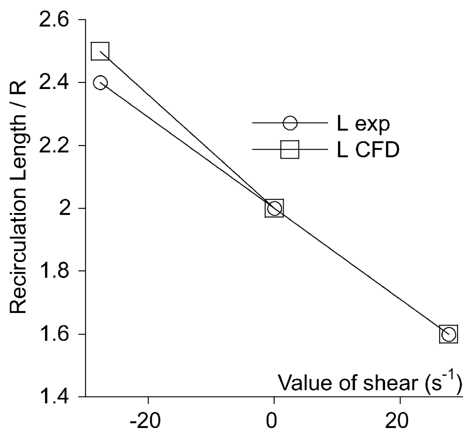

Fig. 8. Measured and computed recirculation lengths for negative, uniform and positive mean shear free-stream distribution.

In order to understand better the mechanism that contributes to the boundary layer development and thus of the appearance of reverse flow for the three cases, a closer examination of the computational results, and in particular of the flow field near the leading edge stagnation point was carried out, Fig. 9. For the cases when shear is present a move of the stagnation point away from the symmetry line is observed. For the case of uniform free-stream velocity distribution the stagnation point is located exactly on the symmetry line (marked with 0 on the vector plot). In the case of positive mean shear the stagnation point moves upwards, towards the

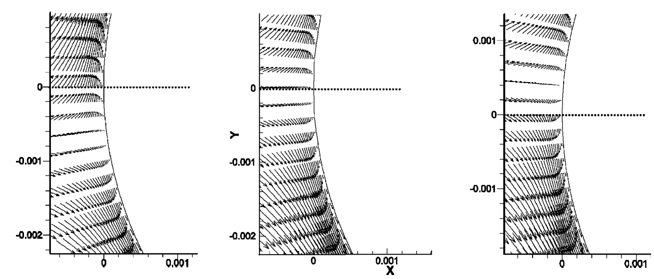

Fig. 9. The leading edge stagnation point location for negative uniform and positive mean shear free-stream velocity distribution. (from left to right). Horizontal dashed line at 0 corresponds to the flat plate symmetry line.

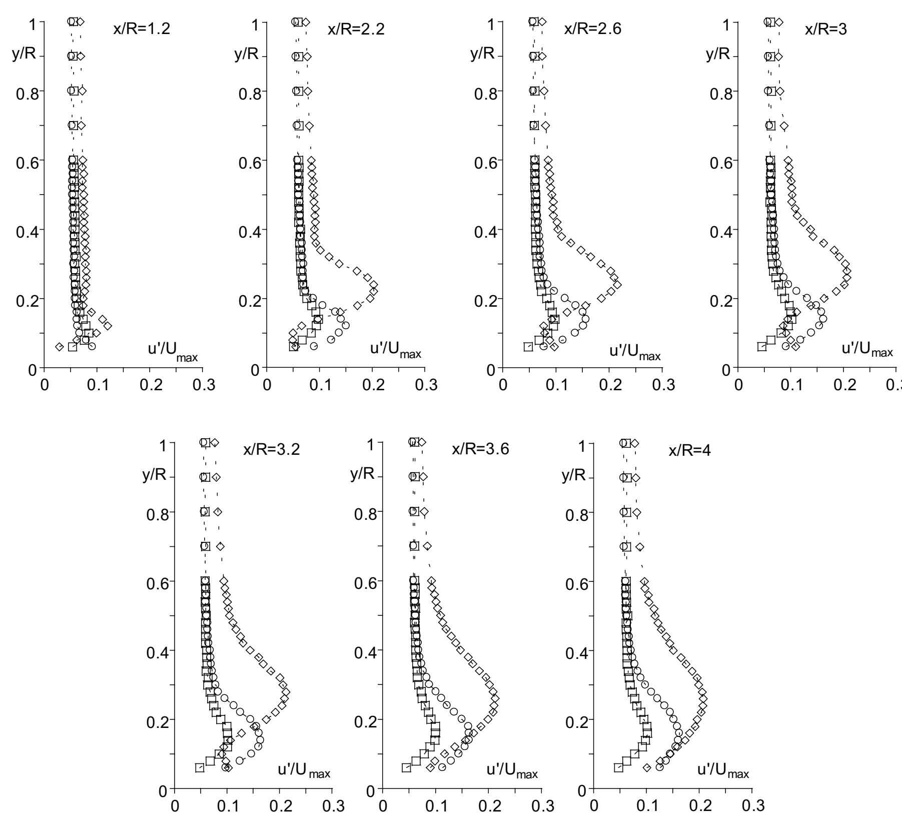

Fig. 10. Comparative diagrams of RMS evolution inside the boundary layer for uniform free-stream inlet velocity distribution (circular symbols), negative mean shear (rhomboid symbols) and positive mean shear (rectangular symbols) free-stream inlet velocity distribution.

high velocity region while in the case of negative shear the stagnation point moves downwards in the opposite direction. This affects the boundary layer development and therefore the length of the reverse flow region on the upper surface of the flat plate. This movement of the stagnation point is one of the major factors affecting the size of the reverse flow region.

In order to see the effect of the longitudinal RMS in the region of the boundary layer on the flow development the u' profiles for all three cases are examined. Fig. 10 shows the evolution of the longitudinal RMS (u') non-dimensionalized by the maximum velocity at the edge of the boundary layer for the three cases and at various stations along the plate. This velocity has been chosen since these RMS distributions correspond to the boundary layer region and thus, the diagrams at each downstream station give a representative straightforward comparative picture of the boundary development for the three cases examined. For all the three cases studied the RMS starts with low values for the first station and its magnitude increases as the boundary layer is separated all the way to the reattachment point. Inside the boundary layer the positive shear gives the lowest RMS values while the negative shear gives the maximum. Transition is accelerated in the case when negative mean shear is present, as strong diffusion of RMS seems to take place in the y direction, normal to the plate, close to the recirculation bubble which though does not extend very far into the flow.

Fig. 11 shows the evolution of the $\overline{u'u'}$ Reynolds stresses along the plate at three normal distances corresponding to $y/R = 7$, 7.5 and 8 respectively from the flat plate surface for all three cases and for a length covering the region of the reverse flow.

These specific distances were selected because they are located well outside the maximum boundary layer thickness that appears for the three cases studied. This is supported by Figs. 1 and 12 where it is shown that the region above $y/R = 7$ is indeed in the free stream region where the velocity gradient is equal to that at the free stream.

One should take note of Fig. 10 where at $y/R = 1$ the RMS for all three cases are nearly the same. Referring to Fig. 11, for each y/R distance the longitudinal Reynolds stresses for all three cases are almost constant along the above region, and within the measurement error of 5%. This result is not a surprise as the fluid in this region comes from an upstream region where the turbulence level is the same, 7%, for all the three cases. As the $\overline{u'u'}$ distributions for the whole area above the reverse flow region are the same, gradients of $\overline{u'u'}$ are also the same and therefore the effect of turbulence transport on the mean flow should be the same for all three cases. The $\overline{u'u'}$ measurements though are not unique representatives of turbulence as they do not provide an indication of the quality of turbulence, i.e. turbulence length scale

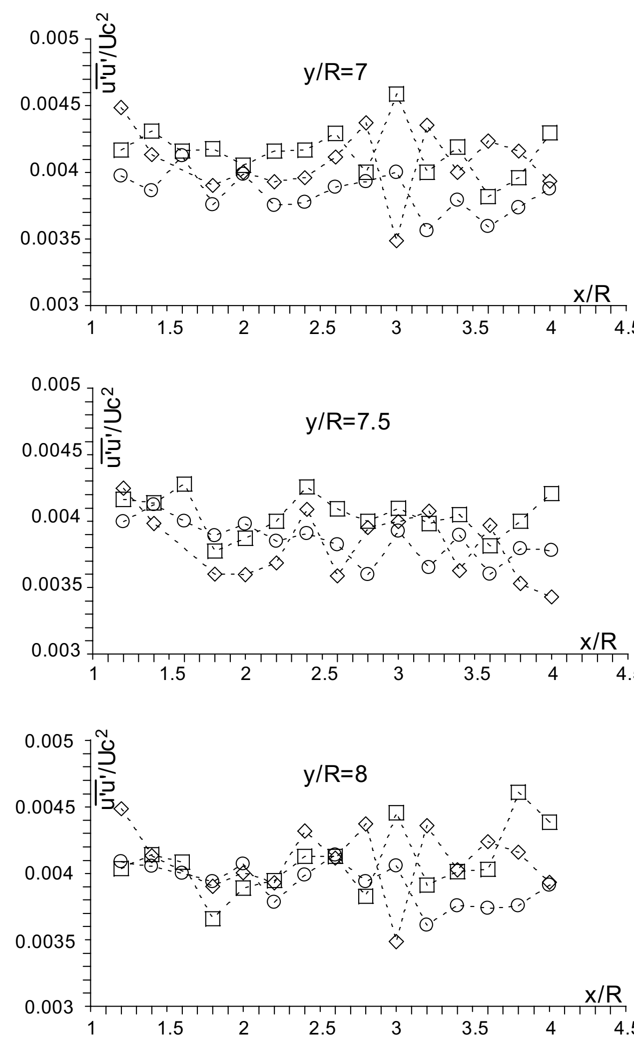

Fig. 11. Longitudinal Reynolds stresses in the free-stream above the reverse flow region at three normal distances for the three cases. Circular symbols: uniform, rectangular: positive mean shear, rhomboid: negative mean shear.

and the presence or not of coherent structures in the flow. The "far-field" longitudinal Reynolds distributions given in Fig. 6 (which are located at $y/R = 15$), show indeed a difference in the initial values of $\overline{u'u'}$ for the two cases when mean shear is present. This difference is due to the mean-shear generator device and in the computational results this is reflected in the different length scales used. So, in the computational results this effect has been taken into account. From the above, one can consider as the major contributor to the boundary layer development the stagnation point move around the leading edge (depending always on the inlet velocity condition) and the consequent lengthening, for a given position, of the boundary layer and the effect, on the initial stages of the boundary layer development, of the curvature of the leading edge. By consequence, the momentum losses due to friction and curvature effects

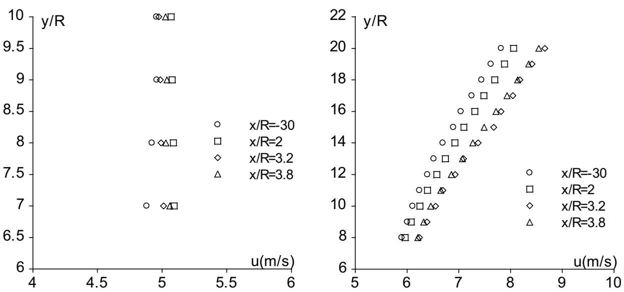

Fig. 12. Velocity distribution in the free-stream region at various stations downstream for uniform and positive mean shear (left and right resp.).

are larger in the presence of negative shear and these losses lead to a larger reverse flow region. This is also substantiated by the observation that beyond the recirculation bubble in the case of negative shear, the extend of high RMS region in the y direction is reduced and it has the same size as the uniform inlet velocity case, despite the fact that it is closer to the fully turbulent boundary layer.

6. Conclusions

The boundary layer development on a flat plate with a semi-circular leading edge (geometry corresponding to the T3L case in ERCOFTAC SIG on transition) under a negative mean shear free-stream inlet velocity distribution is examined experimentally and computationally. The flow development shows a large reverse flow region starting before the first measurement point and develops downstream. The experimental investigation has been supported by a computational procedure using an elliptic Navier–Stokes solver incorporating the non-linear k–ε model of Craft et al. (1996) in its low-Reynolds number formulation. The computational results showed in general a satisfactory agreement with the measured boundary layer velocity profiles, the RMS distributions inside the boundary layer and the integral parameters. In the second part, a comparison is made with the experimental data of two other cases reported by Palikaras et al. (2002) with different inlet conditions, a uniform velocity and a positive mean-shear distribution that has the same absolute value of velocity gradient with the negative one. Concerning the flow development downstream the reattachment point in the case of negative shear, the boundary layer is closer to becoming fully turbulent than the other two cases. This is due to the larger size of the reverse flow region which resulted in higher RMS values within the boundary layer.

In the cases where the mean shear flow is present, and for the same inlet turbulence level at the axis of symmetry, it is shown that the values of the longitudinal Reynolds stresses at the same normal distance from the plate surface, above the boundary edge and in the free-stream region for the three examined cases are almost identical. This is due to the fact that the fluid in this area comes from a region upstream of the plate where the turbulence level is set the same, 7%, for all three cases studied. Therefore the primary mechanism regarding at least the size of the reverse flow region is mainly related to the stagnation point in the region of the leading edge, where there is a move of it from the symmetry line depending on the sign of the imposed shear. As a consequence, larger or smaller momentum losses appear inside the boundary layer, referring always to the same side of the flat plate and thus larger or smaller recirculation zone is detected, when negative or positive shear respectively is imposed.

References

Apsley, D.D., Leschziner, M.A., 1998. A new low-Reynolds-number nonlinear two-equation turbulence model for complex flows. Int. J. Heat Fluid Flow 19, 209–222.

Castro, I.P., Haque, A., 1987. The structure of a turbulent shear layer bounding a separation region. J. Fluid Mech. 179, 439–468.

Chen, W.L., Lien, F.S., Leschziner, M.A., 1998. Non-linear eddy-viscosity modelling of transitional boundary layers pertinent to turbomachinery aerodynamics. Int. J. Heat Fluid Flow 19, 297–306.

Craft, T.J., Launder, B.E., Suga, K., 1996. Development and application of a cubic eddy-viscosity model of turbulence. Int. J. Heat Fluid Flow 17, 108–115.

Lou, W., Hourmouziadis, J., 2000. Separation bubbles under steady and periodic-unsteady main flow conditions. J. Turbomachinery, ASME Trans. 122, 634–643.

Mayle, R.E., 1991. The role of laminar-turbulent transition in gas turbine engine. ASME Gas Turbine Conf. 91-GT-261.

Palikaras, A., Yakinthos, K., Goulas, A., 2002. Transition on a flat plate with a semi-circular leading edge under uniform and positive shear free-stream flow. Int. J. Heat Fluid Flow 23, 455–470.

Rohr, J.J., Itsweire, E.C., Helland, K.N., Van Atta, C.W., 1988. An investigation of the growth of turbulence in a uniform mean-shear flow. J. Fluid Mech. 187, 1–33.

Savill, A.M., 1995. A summary report on the COST ERCOFTAC Transition SIG Project evaluating turbulence models for predicting transition. ERCOFTAC Bull. 24, 57–61.